January 2003

Infrared-active vibron bands associated with substitutional impurities in solid parahydrogen

Robert Hinde
University of Tennessee, rhinde@utk.edu

Recommended Citation

Infrared-active vibron bands associated with substitutional impurities in solid parahydrogen

Robert J. Hinde[a)]

Department of Chemistry, University of Tennessee, Knoxville, Tennessee 37996-1600

We present a model for the line shapes of infrared-active $Q_1(0)$ vibron bands observed in solid parahydrogen doped with low concentrations of spherical substitutional impurities. The line shapes are highly sensitive to the H_2 vibrational dependence of the dopant–H_2 interaction. When this vibrational dependence is strong, the dopant can trap the infrared-active vibron in its first solvation shell; in this case, the trapped vibron manifests itself in the absorption spectrum as a narrow feature to the red of the pure solid's vibron band. © *2003 American Institute of Physics.*
[DOI: 10.1063/1.1584662]

In solid hydrogen and its isotopomers HD and D_2, individual molecules retain good vibrational and rotational quantum numbers (v,j) because the rovibrational coupling terms in the intermolecular potential are much smaller than the rotational and vibrational energy level spacings of individual molecules.[1] The infrared (IR) absorption spectrum of solid H_2 thus exhibits several features that correlate with definite rovibrational molecular excitations.[2–5] These molecular excitations may be accompanied by the creation of one or more phonons; these phonon sidebands, however, are often well separated from the zero-phonon absorption features because solid H_2 has a relatively high Debye frequency.[6]

Because the rovibrational coupling between adjacent molecules is not exactly zero, the zero-phonon features present themselves as exciton bands, with widths of a few wave numbers, in which the rovibrational excitation travels throughout the solid.[7,8] These bands have been recorded at high resolution both in pure solid parahydrogen (pH_2), the ground state of the crystal in which each H_2 molecule has rotational quantum number $j=0$, and in pH_2 solids containing low concentrations of $j=1$ orthohydrogen (oH_2);[3–5,9,10] analysis of the widths and shapes of these bands can provide information about the $H_2–H_2$ intermolecular potential and insight into the exciton dynamics in solid pH_2.[11–13]

A new zero-phonon feature, correlated with the H_2 pure vibrational $Q_1(0)$ transition $(v,j)=(1,0)\leftarrow(0,0)$, appears in the IR absorption spectrum of rapid vapor deposited pH_2 solids containing spherical substitutional impurities such as Ar or Xe atoms.[10,14] In this Communication, we show that this feature is a signature of symmetry breaking by the dopant species, argue that its line shape provides information regarding the solvation of impurities in molecular quantum solids, and develop a simple model that allows this information to be extracted from the absorption spectrum.

Symmetry breaking also gives rise to IR-active absorption features associated with the H_2 $Q_1(0)$ transition in both dense pH_2 gas and bound $(pH_2)_2$ van der Waals dimers.[15] Because pH_2 molecules are spherically symmetric, a pair of

$v=0$ pH_2 molecules exhibits inversion symmetry about the dimer center-of-mass. Vibrationally exciting one of the molecules breaks this symmetry and generates a weak electric dipole moment in the dimer; consequently a nonzero transition dipole moment connects the initial $v=0+v=0$ state and the final $v=0+v=1$ state, and the transition is IR active. This dipole moment arises from overlap interactions between the H_2 molecules and is parallel to the vector connecting the centers-of-mass of the two molecules. Its magnitude decays rapidly as the $H_2–H_2$ separation R increases;[16] hence only R values less than roughly 4 Å contribute significantly to the dimer's IR activity.

The nominal nearest-neighbor distance in solid pH_2 is[1] $R=3.79$ Å, and vibrational excitation of a single molecule in the solid therefore induces weak transition dipole moments in each of its neighbors. The underlying symmetry of the close packed pH_2 crystal lattice, however, eliminates the *net* transition moment associated with $Q_1(0)$ transitions of individual pH_2 molecules, as Fig. 1(a) shows. (Because only nearest-neighbor $v=0+v=1$ pairs make a significant contribution to the net transition moment, any close packed lattice will exhibit this cancellation effect.) Consequently the $Q_1(0)$ feature is absent from the IR absorption spectrum of pure solid pH_2.[10,11,14]

Consider instead a pH_2 solid containing isolated, electrically neutral, spherical substitutional impurities. Suppose that a pH_2 molecule next to an impurity is vibrationally excited. As in the pure solid, this excitation generates weak overlap-induced transition dipole moments in neighboring pH_2 molecules. Overlap interactions between the vibrationally excited pH_2 and the dopant will also generate a weak transition dipole moment. However, because the interaction-induced electrical properties of $pH_2–pH_2$ and dopant–pH_2 pairs differ, the net transition moment associated with the vibrational excitation will be nonzero, as shown in Fig. 1(b). Hence the $Q_1(0)$ excitation of a pH_2 molecule next to the impurity will be IR active. Furthermore, if the substitutional impurity does not disrupt the solid's lattice structure, *only* those pH_2 molecules adjacent to the impurity will be IR ac-

---
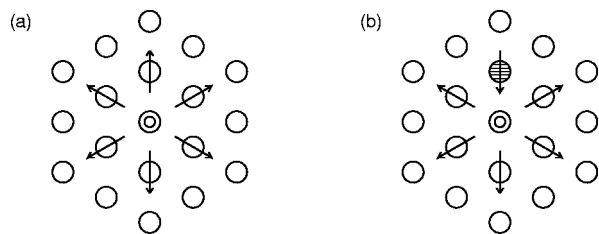
[a)]Electronic mail: rhinde@utk.edu

(a)   (b)

FIG. 1. Vibrational transition dipole moments in pH_2 aggregates. Open single circles represent $v=0$ pH_2 molecules; double circles represent pH_2 molecules undergoing a $v=1 \leftarrow 0$ excitation. (a) In a close packed pure pH_2 solid, excitation of a single pH_2 molecule generates twelve $Q_1(0)$ transition dipole moment vectors, six of which are shown here. The twelve vectors sum to zero because of the underlying symmetry of the close packed lattice. (b) In a pH_2 solid containing a substitutional impurity (shaded circle), excitation of a pH_2 molecule next to the impurity yields a nonzero net $Q_1(0)$ transition dipole moment because dopant–pH_2 and pH_2–pH_2 pairs have different transition moments.

tive, because the overlap interactions that generate the transition moment are short-ranged.

The line shape of the $Q_1(0)$ absorption feature associated with this excitation can be computed from the solid's vibron Hamiltonian, which is well approximated by a tight-binding-like model in which nearest-neighbor pH_2 molecules are coupled by off-diagonal matrix elements that represent the "hopping" of the vibrational excitation from one molecule to the next.[7,17,18] If $|k\rangle$ represents the localized vibrational state in which pH_2 molecule k is vibrationally excited and all other pH_2 molecules are in the vibrational ground state, this model Hamiltonian can be written[18]

$$\hat{H} = \sum_k E_k |k\rangle\langle k| + \lambda \sum_{k,n=\mathrm{nn}} |k\rangle\langle n|, \qquad (1)$$

where E_k is the $Q_1(0)$ transition energy for a vibrational excitation localized on molecule k and λ represents the vibrational coupling between nearest-neighbor (nn) molecules. Intermolecular interactions in the solid[12] reduce E_k from its gas-phase value of $E_k = 4161.1$ cm^{-1} to $E_k = 4152.2$ cm^{-1}. Analysis of the IR absorption spectrum of nearest-neighbor oH_2–oH_2 pairs isolated in solid pH_2 indicates[19] that the hopping parameter $\lambda = -0.225$ cm^{-1}.

In a doped pH_2 crystal, the $Q_1(0)$ transition energy E_k for pH_2 molecules next to an impurity will differ slightly from that for pH_2 molecules distant from the impurity because of differences between the H_2–H_2 and dopant–H_2 potentials. We account for this by introducing a parameter ΔE that quantifies the shift in the $Q_1(0)$ transition energy for pH_2 molecules adjacent to the dopant. For these molecules, $E_k = 4152.2$ cm$^{-1} - \Delta E$; for all other pH_2 molecules, E_k remains at 4152.2 cm^{-1}.

We now use Eq. (1) to predict the line shape of the dopant-induced $Q_1(0)$ vibron feature. This requires us to choose a specific model describing the network of nearest-neighbor interactions in the doped pH_2 solid. An analysis of the IR absorption spectrum of CH_4 dopants in rapid vapor deposited pH_2 solids[20] shows that these solids typically contain both locally face centered cubic and locally hexagonal close packed regions. We therefore treat the doped pH_2 solid

as a random close packed solid consisting of a randomly chosen sequence of close packed planes of H_2 molecules.

To compute the dopant-induced $Q_1(0)$ IR absorption line shape, we model the doped solid using a supercell approach previously applied to the Raman spectrum of mixed oH_2/pH_2 solids,[18] in which a small portion of the solid is carved out from the bulk and replicated in all three directions with periodic boundary conditions. This imposes an artificial periodicity on the model system that is absent from real doped pH_2 solids, which are aperiodic by virtue of their random stacking pattern and the presence of randomly located impurities, and adds spurious fine structure to the vibron band computed here. Although we cannot eliminate this fine structure entirely, we can soften it by combining the results obtained using several supercells with different sizes (and hence different underlying periodicities). Here we choose three roughly cubic supercells containing 4032, 5130, and 6120 molecules, respectively.

We designate N_d randomly selected lattice sites in each supercell as dopants. We choose N_d values that give an impurity mole fraction of roughly 0.1% for each box, which is comparable to the dopant concentrations that have been achieved experimentally.[10,14] At these low impurity concentrations the dopants are well isolated from each other and no pH_2 molecule has more than one impurity as a neighbor.

We then construct the Hamiltonian matrix for a given supercell using Eq. (1) and diagonalize it to obtain the eigenvectors representing the doped crystal's vibrons. These eigenvectors are linear combinations of the localized vibrational states $|k\rangle$

$$\Psi_n = \sum_k C_{k,n} |k\rangle. \qquad (2)$$

The coefficients $C_{k,n}$ determine the $Q_1(0)$ transition dipole moment $\mathbf{M}_n$ associated with the vibron Ψ_n through the equation

$$\mathbf{M}_n = M_0 \sum_{d,k=\mathrm{nn}} C_{k,n} \mathbf{U}_{k,d}, \qquad (3)$$

which is a double summation over nearest-neighbor pairs of dopants d and pH_2 molecules k. In this equation, $\mathbf{U}_{k,d}$ is the unit vector from pH_2 molecule k to dopant d and M_0 represents the magnitude of the transition dipole moment associated with the localized vibrational excitation of a pH_2 molecule adjacent to a dopant. The quantity $M_0 \mathbf{U}_{k,d}$ in Eq. (3) is simply the sum of the twelve transition dipole moment vectors associated with the localized $Q_1(0)$ excitation of molecule k next to dopant d. Six of these vectors are shown in Fig. 1(b); six others are associated with pH_2 molecules in neighboring lattice planes. If the underlying close packed lattice structure is preserved in the doped solid, this sum must be aligned with the vector $\mathbf{U}_{k,d}$ whether sites d and k are in the same lattice plane, as shown in Fig. 1(b), or in adjacent lattice planes.

Finally, we obtain a theoretical dopant-induced $Q_1(0)$ line shape by weighting the eigenvalues of the vibron Hamiltonian by their respective $|\mathbf{M}_n|^2$ values and convolving the resulting stick spectrum with a Lorentzian broadening function with full width at half maximum of 0.01 cm^{-1}. We av-
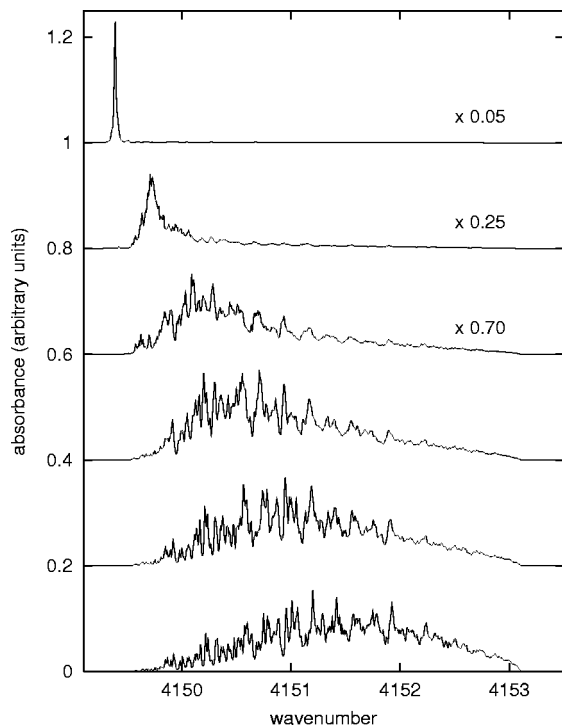
FIG. 2. Theoretical dopant-induced pH_2 $Q_1(0)$ absorption spectra for several values of the detuning parameter ΔE. From bottom to top, $\Delta E = 0.25$, 0.5, 0.75, 1, 1.5, and 2 cm^{-1}. The spectra are offset vertically for clarity. Note that the spectra for $\Delta E \geqslant 1$ cm^{-1} have been reduced in intensity for ease of presentation.

erage together 15 such features, each with a different underlying random stacking pattern, to produce the absorption spectra shown here. Five features are computed for each of the three supercells, and the contributions from each supercell are normalized to a dopant mole fraction of 0.1%.

Figure 2 shows the resulting spectra for detuning parameters ΔE ranging from 0.25 to 2 cm^{-1}. The spectra are shown in reduced absorbance units, in which we choose $M_0 = 1$ for all dopants. (The actual magnitude of M_0 for Ar-doped pH_2 is estimated below.) For comparison, Fig. 3 shows the total vibron density of states for $\Delta E = 0.5$ cm^{-1}; the densities of states for other values of ΔE are very similar to the plot shown there. A comparison of Fig. 3 with the vibron density of states computed for pure pH_2 in Ref. 8 shows that remnants of the spurious fine structure described above persist, even after results from the three supercells are
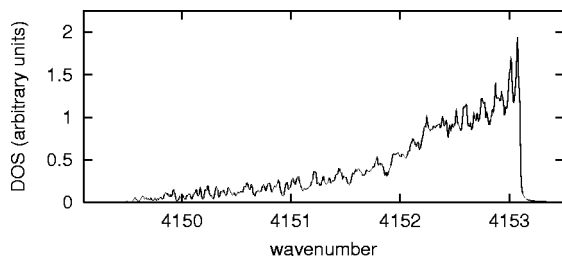

FIG. 3. Vibron density of states (DOS) for random close packed solid pH_2 with a dopant concentration of 0.1% and $\Delta E = 0.5$ cm^{-1}. The DOS has been convolved with a 0.01-cm^{-1} Lorentzian broadening function.

combined. The fine structure observed in the absorption spectra presented in Fig. 2 is seen to correlate with this spurious fine structure in the vibron band.

At low values of the detuning parameter ΔE, the dopant-induced $Q_1(0)$ absorption feature shows substantial IR intensity over the entire vibron band ranging from $\tilde{\nu} = 4149.5$ cm^{-1} to $\tilde{\nu} = 4153.1$ cm^{-1}. As ΔE increases, the dopant-induced absorption feature shifts to the red and sharpens; for $\Delta E = 2$ cm^{-1} the feature's full width at half maximum is only 0.02 cm^{-1}. The integrated intensity of the dopant-induced feature remains constant as ΔE changes; as a consequence, the narrow features observed for large ΔE have much higher peak intensities than the broad features observed for small ΔE. The overall shape of the $\Delta E = 0.25$ cm^{-1} absorption feature is very similar to that observed experimentally for Ar-doped solid pH_2,[10] while the narrow absorption feature observed for $\Delta E = 2$ cm^{-1} is reminiscent of, although slightly broader than, the narrow $Q_1(0)$ features induced by spherical $j = 0$ HCl and DCl dopants in solid pH_2.[21]

The evolution in the shape of the dopant-induced feature as the detuning parameter increases reflects a transition from a delocalized IR-active vibron at small ΔE to a strongly localized IR-active vibron at large ΔE. As ΔE increases, it becomes more and more difficult for a vibrational excitation localized in the dopant's first "solvation shell" to hop away from the dopant, and the vibrational coordinates of pH_2 molecules in this solvation shell, which are the only IR-active molecules in the solid, become effectively decoupled from the rest of the system.

The impurity-induced $Q_1(0)$ absorption features shown in Fig. 2 differ qualitatively from the oH_2-induced $Q_1(0)$ absorption feature studied elsewhere.[3,11] The oH_2-induced feature arises from $Q_1(0)$ transition moments induced in pH_2 molecules by the quadrupolar electrostatic field of the oH_2 dopant.[11] This particular induction mechanism gives the oH_2-induced $Q_1(0)$ feature a characteristic asymmetric shape[3,10] with peak absorption intensity at $\tilde{\nu} = 4153.1$ cm^{-1}, at the blue edge of the vibron band shown in Fig. 3. By comparison, the dopant-induced $Q_1(0)$ features in Fig. 2 are relatively weak at the upper end of the vibron band, even though the vibron density of states is largest there. This is simply an indication that the vibrons that become IR active due to the presence of a spherical substitutional impurity have different symmetry characteristics from those vibrons that are activated by the anisotropic quadrupolar field of oH_2 dopants.

To show that the mechanism described here can produce dopant-induced $Q_1(0)$ features of measurable intensity, we estimate the magnitude of the transition moment M_0 in Eq. (3) for Ar-doped solid pH_2 at $T = 4$ K. This estimate is derived from discrete-time constant-volume path integral Monte Carlo simulations[22] of an isolated Ar dopant embedded in a hexagonal close packed solid containing 179 pH_2 molecules. These simulations employ pairwise-additive transition dipole moments[16,23] and potentials[1,24] and represent each particle by a 64-bead ring polymer; simulations using 32-bead polymers give very similar results. From these simulations, we estimate that $|M_0| = 0.6 \pm 0.1$ millidebye for pH_2

molecules adjacent to the Ar impurity. For comparison, the average quadrupole-induced $Q_1(0)$ transition moment for pH_2 molecules next to oH_2 dopants[11] is 0.2 millidebye. The overlap-induced IR absorption features discussed here should thus be comparable in intensity to the quadrupole-induced $Q_1(0)$ absorption feature observed in oH_2-doped solid pH_2.[3,10,11]

In summary, we have presented a microscopic model for the IR-active $Q_1(0)$ vibron bands of solid pH_2 doped with spherical substitutional impurities. The impurities induce IR activity in neighboring pH_2 molecules via short-range overlap interactions. Our model incorporates a single adjustable parameter: the vibrational detuning ΔE for pH_2 molecules in the impurity's first solvation shell. The shape of the dopant-induced $Q_1(0)$ absorption feature is a sensitive probe of the magnitude of ΔE. For small values of ΔE, the dopant-induced absorption feature is broad and nearly symmetrical, like that observed in Ar-doped solid pH_2.[10] As ΔE increases, the absorption feature becomes asymmetrical and shifts to the red. For large (but not unrealistically large) values of ΔE, the vibrational coordinates of the pH_2 molecules in the dopant's first solvation shell decouple from the bulk solid's vibron band. The dopant-induced $Q_1(0)$ absorption feature then collapses into a narrow peak to the red of the pure solid's vibron band, like that observed in HCl- and DCl-doped solid pH_2.[21]

The value of ΔE that is appropriate for a particular dopant is determined by the dependence of the dopant–pH_2 potential on the pH_2 vibrational coordinate, once this potential is averaged over the distribution of intermolecular distances characteristic of nearest neighbors in the pH_2 solid. Inspection of the relevant potentials[24] suggests that for rare gas dopants ΔE should increase monotonically on going from Ar to Kr to Xe, and that these atoms should fit comfortably into single substitutional sites in the pH_2 lattice. High-resolution IR absorption studies of pH_2 solids doped with these rare gases could therefore help confirm the validity of the model presented here.

[1] I. F. Silvera, Rev. Mod. Phys. **52**, 393 (1980).
[2] T. Oka, Annu. Rev. Phys. Chem. **44**, 299 (1993).
[3] R. A. Steinhoff, K. V. S. R. Apparao, D. W. Ferguson, K. N. Rao, B. P. Winnewisser, and M. Winnewisser, Can. J. Phys. **72**, 1122 (1994).
[4] M. Mengel, B. P. Winnewisser, and M. Winnewisser, Phys. Rev. B **55**, 10420 (1997).
[5] M. Mengel, B. P. Winnewisser, and M. Winnewisser, J. Mol. Spectrosc. **188**, 221 (1998).
[6] K. Carneiro and M. Nielsen, in *Anharmonic Lattices, Structural Transitions, and Melting*, edited by T. Riste (Noordhoff, Leiden, 1974).
[7] J. Van Kranendonk, Physica (Amsterdam) **25**, 1080 (1959).
[8] S. K. Bose and J. D. Poll, Can. J. Phys. **68**, 159 (1990).
[9] W. Ivancic, T. K. Balasubramanian, J. R. Gaines, and K. N. Rao, J. Chem. Phys. **74**, 1508 (1981).
[10] R. J. Hinde, D. T. Anderson, S. Tam, and M. E. Fajardo, Chem. Phys. Lett. **356**, 355 (2002).
[11] V. F. Sears and J. Van Kranendonk, Can. J. Phys. **42**, 980 (1964).
[12] J. Van Kranendonk and G. Karl, Rev. Mod. Phys. **40**, 531 (1968).
[13] R. M. Dickson and T. Oka, J. Phys. Chem. **99**, 2617 (1995).
[14] M. E. Fajardo and S. Tam, J. Chem. Phys. **108**, 4237 (1998).
[15] A. R. W. McKellar, J. Chem. Phys. **92**, 3261 (1990).
[16] W. Meyer, A. Borysow, and L. Frommhold, Phys. Rev. A **40**, 6931 (1989).
[17] H. M. James and J. Van Kranendonk, Phys. Rev. **164**, 1159 (1967).
[18] J. L. Feldman, J. H. Eggert, J. De Kinder, R. J. Hemley, H.-k. Mao, and D. Schoemaker, Phys. Rev. Lett. **74**, 1379 (1995).
[19] Y. Zhang, T. J. Byers, M.-C. Chan, T. Momose, K. E. Kerr, D. P. Weliky, and T. Oka, Phys. Rev. B **58**, 218 (1998).
[20] S. Tam, M. E. Fajardo, H. Katsuki, H. Hoshina, T. Wakabayashi, and T. Momose, J. Chem. Phys. **111**, 4191 (1999).
[21] D. T. Anderson, R. J. Hinde, S. Tam, and M. E. Fajardo, J. Chem. Phys. **116**, 594 (2002).
[22] R. P. Feynman and A. R. Hibbs, *Quantum Mechanics and Path Integrals* (McGraw-Hill, New York, 1965).
[23] A. M. Dunker and R. G. Gordon, J. Chem. Phys. **68**, 700 (1978).
[24] R. J. Le Roy and J. M. Hutson, J. Chem. Phys. **86**, 837 (1986).